Inorg. Chem. **2004**, *43*, 7656–7664

Structure of YAG Crystals Doped/Substituted with Erbium and Ytterbium

Łukasz Dobrzycki,[†] Ewa Bulska,[†] Dorota Anna Pawlak,[‡] Zygmunt Frukacz,[‡] and Krzysztof Woźniak*,[†]

Chemistry Department, Warsaw University, ul. Pasteura 1, 02-093 Warszawa, Poland, and Institute of Electronic Materials Technology, ul. Wolczynska 133, 01-919 Poland

Received January 19, 2004

Two series of yttrium aluminum garnets doped with erbium and ytterbium ions have been studied by single-crystal X-ray diffraction. The single crystals were obtained by the Czochralski method. The concentration of doping ions was established by the plasma emission spectroscopy method. For the Er series, it is equal to 23.4, 46.7, 72.5, and 100%, whereas, for Yb-doped YAGs, it equals 26.5, 48.2, 75.9, and 100%. The results are supplemented by the data obtained for pure YAG. The X-ray data for all samples were collected at two temperatures: 295(2) and 102(2) K. Additionally, for YAGs doped with ca. 50% of doping ions, some more detailed temperature measurements were performed. Pure single crystals of ErAG and YbAG were also studied as a function of diffraction angles. Careful single-crystal measurements utilizing a CCD diffractometer revealed the unit cell parameters, which slightly—but significantly—deviate from cubic symmetry. The average unit cell parameters change linearly with the amount of substituting Er and Yb cations, with two different slopes related to the ionic radii. Both of the dodecahedral distances depend linearly on the concentration of the substituting ions, but the longer dodecahedral distance also changes with temperature contrary to the shorter one. There is no correlation between the octahedral interatomic distance [Al(VI)···O] and the unit cell parameter or temperature; however, weak trends appear for the tetrahedral [Al(IV)···O] distance. Such weak trends are just the secondary consequences of the ion substitution taking place at the dodecahedral site. The dependences between the unit cell parameters and the concentration of doping ions allow us to establish concentrations of particular doping ions in mixed (Er, Yb) doped YAGs just on the basis of the measured unit cell parameters and knowledge of the amount of Y.

Introduction

Garnet is the common name of minerals belonging to the orthosilicate group, which contain isolated $[SiO_4]^{4-}$ ions. The general chemical formula of garnets is $C_3A_2D_3O_{12}$. In the case of natural garnets, it can be written as $C_3A_2[SiO_4]_3$, where usually C = Fe^{2+}, Mg^{2+}, Mn^{2+}, and Ca^{2+} and A = Al^{3+}, Fe^{3+}, Cr^{3+}, and V^{3+}. Garnets crystallize in the most symmetric space group, $Ia\bar{3}d$, of the cubic crystal system. In the garnet structure C denotes a large ion located at dodecahedral sites (coordination number (CN) = 8), A stands for a medium size ion at octahedral sites (CN = 6), and D denotes a relatively small ion located at tetrahedral sites (CN = 4; see Figure 1).

Doped yttrium aluminum garnets (YAGs) are widely used materials for solid-state lasers. Crystalline YAG is an excellent matrix for active ions such as lanthanides (Ln).

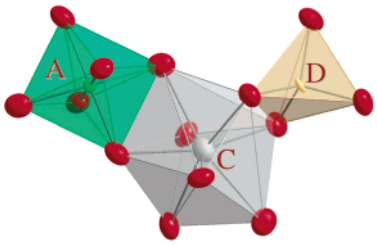

Figure 1. Coordination polyhedra in the garnet structure presented as three-dimensional atomic displacement ellipsoids of ions in Yb:YAG crystal at T = 295 K.

The crystal structure of YAG is illustrated in Figure 1S (Supporting Information).

There were a few papers published about a possible distortion of the garnet structure from the ideal cubic system. In the low-temperature diffraction data, two reflections [222] and [666] were found which cannot correspond to the $Ia\bar{3}d$ space group.[1,2] The change of position of the lanthanide ions from the dodecahedral sites to the octahedral ones is a possible explanation of the above observation.[3] As a result

* Author to whom correspondence should be addressed. E-mail: kwozniak@chem.uw.edu.pl.
[†] Warsaw University.
[‡] Institute of Electronic Materials Technology.

10.1021/ic049920z CCC: $27.50
Published on Web 10/15/2004

some changes of stoichiometry should be observed. This effect was connected also with the size of the lanthanide ion at the dodecahedral positions. For example, a $Pr_3Ga_5O_{12}$ crystal should be perfectly stoichiometric (because of the large ionic radius of the praseodymium ion), whereas a $Lu_3Ga_5O_{12}$ crystal should contain a quite substantial additional amount of lutetium ions. In any of these papers, the authors did not take into account a possibility of multiple reflections, which could also rationalize the presence of these two above-mentioned reflections. Another explanation of their presence could be a nonspherical distribution of electron density in the crystal.

Some of the characteristics of garnets distinguished in the [111] crystallographic direction are related to lanthanide ions substituting octahedral sites located exactly along the [111] direction.[4−6] Unfortunately, it is very difficult to see the distortion of YAGs from the cubic structure by diffraction methods, when it is quite small. However, it was found with EXAFS that ca. 10% of atoms from the dodecahedral sites relocate to the octahedral sites. And the atoms from the octahedral sites locate at the dodecahedral sites.[7] Calculating per unit cell, ca. 2 atoms exchange their positions. It was also found that garnets stay stoichiometric. In the $Ia\bar{3}d$ space group, there are four 3-fold axes along the space diagonals. The exchange of the ions between dodecahedral and octahedral sites destroys the $\bar{3}$-fold symmetry in the space diagonal directions of the cubic system. The symmetry is lowered. It was suggested that it is lowered to the trigonal system, space group $R\bar{3}$.[2] This is equivalent to elongation of the cube along, for example, the [111] direction. This would be in a good agreement with the experimental facts suggesting a different behavior of garnets along the {[111]} crystallographic directions. After such transformation, from space group $Ia\bar{3}d$ to $R\bar{3}$, coordinates for all positions except the octahedral ones stay the same.[7]

A detailed statistical analysis of the relations between different geometrical parameters of garnets is described in ref 8. It also contains most of the references to the structures of garnet crystals refined so far. They were studied using a number of different techniques such as single-crystal and powder X-ray and neutron crystallography, NMR, XPS, and other spectroscopic methods.[9−11]

The minimum concentration of doping agent required to obtain laser activity usually is quite low (a few percent or less), so structural changes caused by such a very low doping level are not easy to detect. We decided to focus our attention on the consequences of doping. To magnify structural effects on doping/substitution, we have chosen as doping ions erbium and ytterbium, which can fully substitute yttrium at its dodecahedral site.

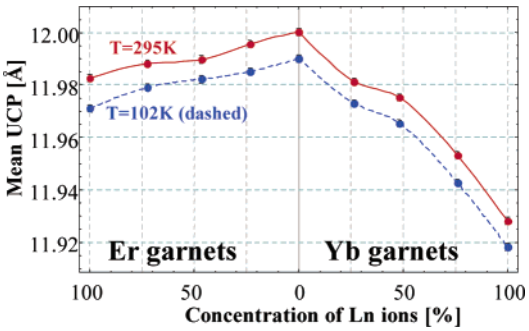

Figure 2. Averaged cubic unit cell edge length vs concentration of the lanthanide Er and Yb ions at 102(2) and 295(2) K.

In this paper we look for the distortion of the YAG structure from the cubic system, for relations between structural parameters characterizing YAG structures, and for the influence of measurement conditions on them. To achieve these aims, we have grown and studied two series of single crystals of YAG doped with Er and Yb ions at the dodecahedral sites. For both series, the amount of substituting lanthanide ions was planned to be 0%, 25%, 50%, 75%, and 100%. Erbium and ytterbium ions were chosen as the dopants because their ionic radii are very similar to the ionic radius of the yttrium ion. This allows even full replacement of yttrium in the garnet structure.

Results and Discussion

The real concentration of lanthanide ions in the crystals was determined by ICP AES. In the Er-doped series the concentration of erbium is equal to 0, 23.4, 46.7, 72.5, and 100 at. %, whereas, for Yb-doped crystals, the concentration of ytterbium amounts to 0, 26.5, 48.2, 75.9, and 100 at. %. For all samples, the crystal structures were refined at two different temperatures: 295 and 102K. For YAG:Er (50 at. %) and YAG:Yb (50 at. %) some additional measurements at 150, 200, and 250 K were carried out. The most important crystal data are given in Table 1S (Supporting Information) together with the refinement details.

As we can see from Table 1S (Supporting Information) and Figure 2, the averaged unit cell parameters change almost linearly with the change of the concentration of doping/substituting ions. Of course, the variation of the average unit cell parameter for the Yb series is larger than for the Er one. The erbium ion (Er^{3+}_{VIII} = 1.004 Å) has an ionic radius similar to yttrium (Y^{3+}_{VIII} = 1.019 Å), which it substitutes. Therefore, the changes in the YAG structure made by erbium are small. The difference between the ytterbium (Yb^{3+}_{VIII} = 0.985 Å) and yttrium ion radii is bigger,[12] so the changes caused by doping with this ion are more significant. In both, the unit cell length decreases with increasing doping level

(1) Popma, T. J. A.; Van Diepen, A. M.; Robertson, J. M. *Mater. Res. Bull.* **1974**, *9*, 699.
(2) Chenevas, J.; Joubert, J. C.; Marezio, M. *J. Less-Common Met.* **1978**, *62*, 373.
(3) Brandle, C. D.; Barns, R. L. *J. Cryst. Growth* **1974**, *26*, 169.
(4) Cohen, R. L. *Phys. Lett.* **1963**, *5*, 177.
(5) Boebeck, A. H.; Spencer, E. G.; Van Uitert, L. G.; Abrahams, S. C.; Barns, R. L.; Grodkiewicz, W. H.; Sherwood, R. C. P.; Schmidt, H.; Smith, D. H.; Walters, E. M. *Appl. Phys. Lett.* **1970**, *17*, 131.
(6) Struve, B.; Huber, G. *Appl. Phys. B* **1985**, *36*, 195.
(7) Dong, J.; Lu, K. *Phys. Rev. B.* **1990**, *43*, 8808.
(8) Pawlak, D.; Wozniak, K.; Frukacz, Z. *Acta Crystallogr. B* **1999**, 55, 736 and references therein.
(9) Etchsmann, B.; Streltsov, V; Ishizawa, N; Maslen, E. N. *Acta Crystallogr. B* **2001**, *57*, 136.
(10) Vosegaard, T.; Byriel, I. P.; Pawlak, D. A.; Wozniak, K.; Jakobsen, H. J. *J. Am. Chem. Soc.* **1998**, *120*, 7900.
(11) Pawlak, D. A.; Wozniak, K.; Frukacz, Z.; Barr, T. L.; Fiorentino, D.; Seal, S. *J. Phys. Chem. B* **1999**, *103*, 1454.
(12) Shannon, R. D. *Acta Crystallogr., Sect. A* **1976**, *32*, 751.

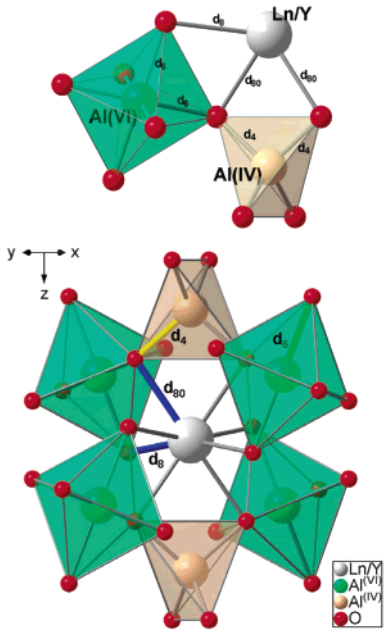

Figure 3. Definition of the most important interatomic distances in the YAG structure.

because of the smaller ionic radii of the doping ions compared to the radius of the host ion. There is also a significant temperature effect (ca. 0.0001 Å/°C) on the variation of the averaged unit cell parameter.

Distortion from Ideal Cubic Symmetry. The unit cell parameters, lengths, and angles, obtained directly from measurements without any averaging, are not equal to one another—as should be the case for the cubic crystal system (Table 2S, Supporting Information)—even when the error bars are taken into account. The unit cell parameters were established on the basis of all reflections measured for a given sample. Although the unit cell lengths (*a*, *b*, *c*) seemed to be different in all cases of doping and also at both temperatures, we have checked, using X-ray powder methods and also thin frame single-crystal CCD measurements, that the deviations from the cubic system are not significant.

To confirm a possible lower symmetry of YAG crystals another very sensitive nondiffraction technique should be applied. The deviations observed from cubic symmetry are too small for diffraction techniques and cannot be uniquely interpreted.

Interatomic Distances. The variation of the unit cell parameters can be decomposed into contributions coming from changes of particular interatomic distances or even into contributions from particular coordinates of the only independent ion in this structure—the oxygen anion. All interatomic distances characterizing the garnet structure are defined in Figure 3. In practice, there are four important distances: the shorter and longer cation−oxygen ion distances of the dodecahedral site (d_{80} and d_8, respectively) and the cation−oxygen ion distances for the octahedral and tetrahedral sites (d_6 and d_4, respectively).

The numerical values of the geometrical parameters are given in Table 3S (Supporting Information). It appears that the shorter d_{80} bond, in principle, does not depend on

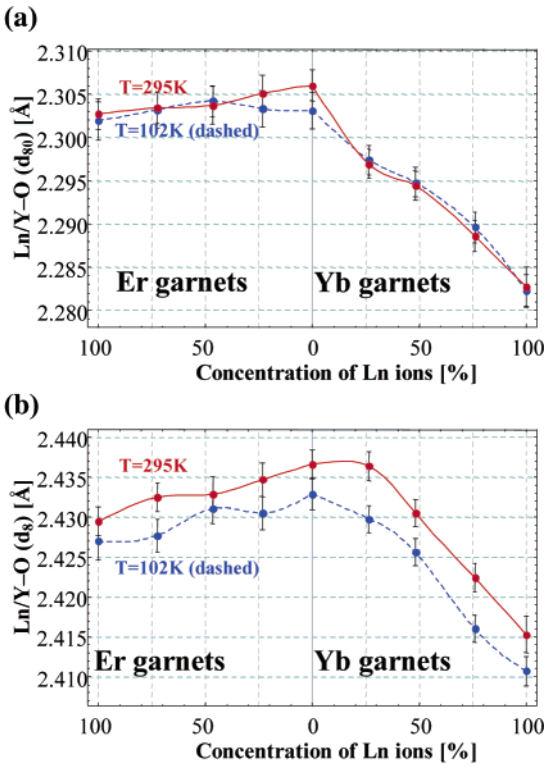

Figure 4. Dependence on concentration for the lanthanide Er and Yb ions at two different temperatures (102, 295 K) of (a) d_{80} (shorter Ln/Y···O distance) and (b) d_8 (the longer Ln/Y···O distance).

temperature contrary to the longer and weaker d_8 bond (Figure 4). The length of d_8 decreases with the increase of the Er ion concentration and ranges from 2.437 Å (2.433 Å at 102 K for YAG) to ca. 2.430 Å (2.427 Å at 102 K for pure ErAG). The range of variation for Yb doped garnets is bigger.

In this case d_8 changes from 2.438 Å (2.433 Å at 102 K) for YAG to 2.415 Å (2.411 Å at 102 K) for pure YbAG. The differences in the values for different garnets are directly related to the differences of ionic radii of Ln/Y ions. For both series the shorter d_{80} distance also changes in the same way as the longer one, d_8, but the range of the changes is smaller. The difference of d_8 at room temperature and at 102 K is almost constant for all samples and amounts to ca. 0.0025 Å, which gives an idea of the temperature effect.

There is not a significant correlation between the d_6 interatomic distance [Al(VI)···O] and the unit cell parameter or temperature. A similar effect was reported in ref 8. The d_6 parameter seems to change in a regular way only in the series of garnets where the octahedral or tetrahedral sites are doped. A stronger trend appears for the distance d_4 [Al(IV)···O], which seems to be dependent on concentration and temperature, even in the case when only an ion at the dodecahedral site is changed. The oxygen ions forming tetrahedra are connected with the cation at the dodecahedral site by two d_{80} edges. However, there are two different kinds of edges for octahedra—one shorter, d_{80}, and one longer, d_8. This is the reason the influence on the d_6 distance is a sum of two different effects. For the last two distances their possible dependences on concentration or temperature are

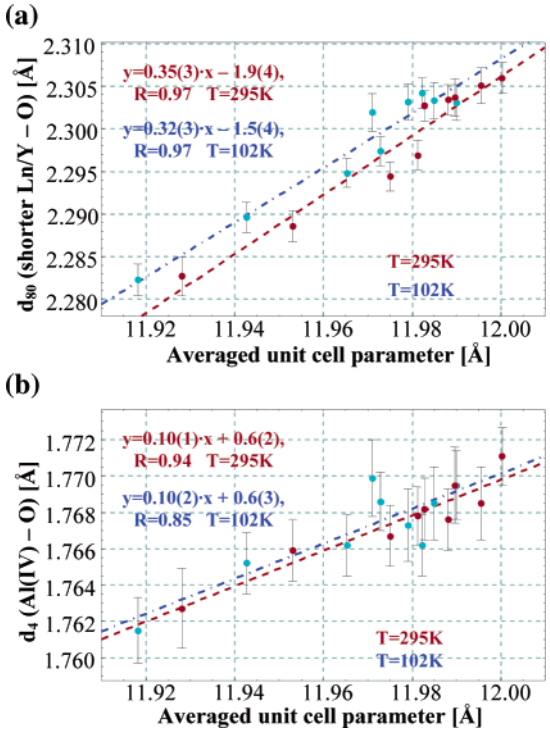

Figure 5. Dependence of (a) d_{80} (shorter Ln/Y···O) and (b) d_4 (Al(IV)···O) distances on the averaged unit cell parameters.

just a secondary consequence of substitution taking place at the dodecahedral site. Such consequences are attenuated as a function of separation from the substitution site.

Some of the interatomic distances correlate well with the average unit cell parameter (Figure 5). In particular the strongest correlation exists for both dodecahedral parameters. There is a weaker relation for the tetrahedral parameter and no relation for the octahedral one.

Oxygen Ion Position. There is a dependence of the absolute distance of the oxygen ion (coordinates times the unit cell parameter, *da*) from the origin of the unit cell, (000), on the concentration of the doping/substituting ions. This relation is very similar to the dependence of the averaged unit cell parameter on the concentration of dopant (Figure 2). This is expected because oxygen is the only atom occupying a general position in the independent part of the unit cell.

Deformation of Ideal Coordination Polyhedra. Departure from the ideal figures was defined by Euler and Bruce[13] by two angles, σ and ϕ, shown in Figure 6. The angle σ is defined by the following equation:

$$\cos(\sigma) = \frac{(x_0 + y_0 + z_0)}{\sqrt{3}\sqrt{(x_0^2 + y_0^2 + z_0^2)}}$$

Here, x_0, y_0, z_0 are coordinates of the oxygen ion from the closest surrounding of Al(VI) at the (000) position. In the case of the ideal octahedron, the σ_o angle is equal to 54.74°, whereas, for the ideal tetrahedral coordination, the angle ligand−the central ion−ligand should be equal to $2\sigma_o$. Additionally, the angle ϕ describing rotation of a given octahedron around the inverse 3-fold axis from the $(1\bar{2}1)$ plane should be equal to 0°. The angle ϕ is defined as the torsion angle between planes on the basis of the following points: $\bar{1}01$, 111, 000; 000, 111, $x_0y_0z_0$. It appears that σ_o depends on the concentration of the doping ion similarly as other parameters. There is a weak dependence for the Er series and a stronger one for the Yb series. For the Er garnets the change of σ is very small: between 52.35 and 52.40°. For Yb garnets, this parameter changes from 52.08 to 52.40°. The ϕ angle is almost constant for the Er-substituted YAGs (3.18−3.08°) and slightly decreasing for the Yb series (3.40−3.18°) with the increasing concentration of Yb ions. Generally, the deviation of the σ_o angle from the ideal octahedral value is around 2.5° in the garnets studied, while the value of the ϕ angle differs by more then 3°. This is in good agreement with the values of these parameters obtained for aluminum garnets presented in ref 13.

Atomic Displacement Parameters. Atomic displacement parameters (ADPs) are the most sensitive parameters to small changes of experimental conditions, especially when there is a loss of intensity of reflections caused by high absorption and/or fluorescence (for pure YAG, for example). But even with these disadvantages we obtained reasonably good data for most of the samples. They are collected in the CIF files attached to this publication in the Supporting Information.

The shape and size of ADPs of the cations are temperature dependent and related to the coordination number of the cations. In the case of aluminum ions some ADPs obtained from unconstrained refinement tend to be small and even negative (nonphysical; see Figure 7)—this is the case for Al at the octahedral site at 100 K in three samples containing a high amount of Yb. However, all such values of ADPs could also be treated as small and positive within the level of errors. But because we do not see any significant differences in the final results of refinement when the ADPs are constrained to be small and positive, and we see regular trends for them when they are unconstrained, we have decided to quote the unconstrained values.

Although the ADPs are positive for Al cations at the tetrahedral sites in all mixed Y/Yb garnets at 100 K—and for the sample containing ca. 50 at. % of Yb for all temperatures—they have an elongated shape in one direction. This can be related to the type and shape of the structural voids occupied by the aluminum ions. The octahedral site more resembles a sphere than the tetrahedral one, so the ADPs of Al(VI) have a more isotropic shape, contrary to Al(IV) which should have its ADPs more flattened in one direction and elongated in the orthogonal ones. The shape of the ADPs is shown in Figure 7. It appears that, for low temperatures, thermal motions of Al ions become hard to detect especially for smaller and more dense structures containing Yb at the dodecahedral site.

Easily vibrating oxygen ions decrease the ADP values of the relatively light aluminum ions, contrary to the cations at the dodecahedral sites (Y, Er, or Yb ions), which are less influenced by these vibrations. The mean values of ADPs, equivalent temperature factors, confirm well the correlation between the motions of the not too heavy ions (Al, O),

(13) Euler, F.; Bruce, J. A. *Acta Crystallogr.* **1965**, *19*, 971.

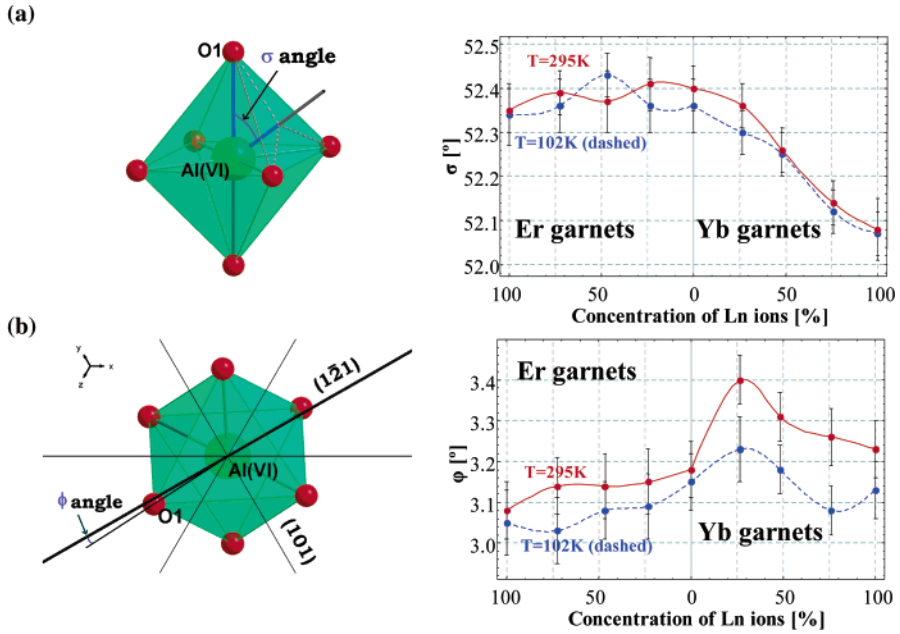

Figure 6. Polyhedron deformation figures and cubic spline lines describing their dependencies on concentration and temperature: (a) ϕ angle; (b) σ angle.

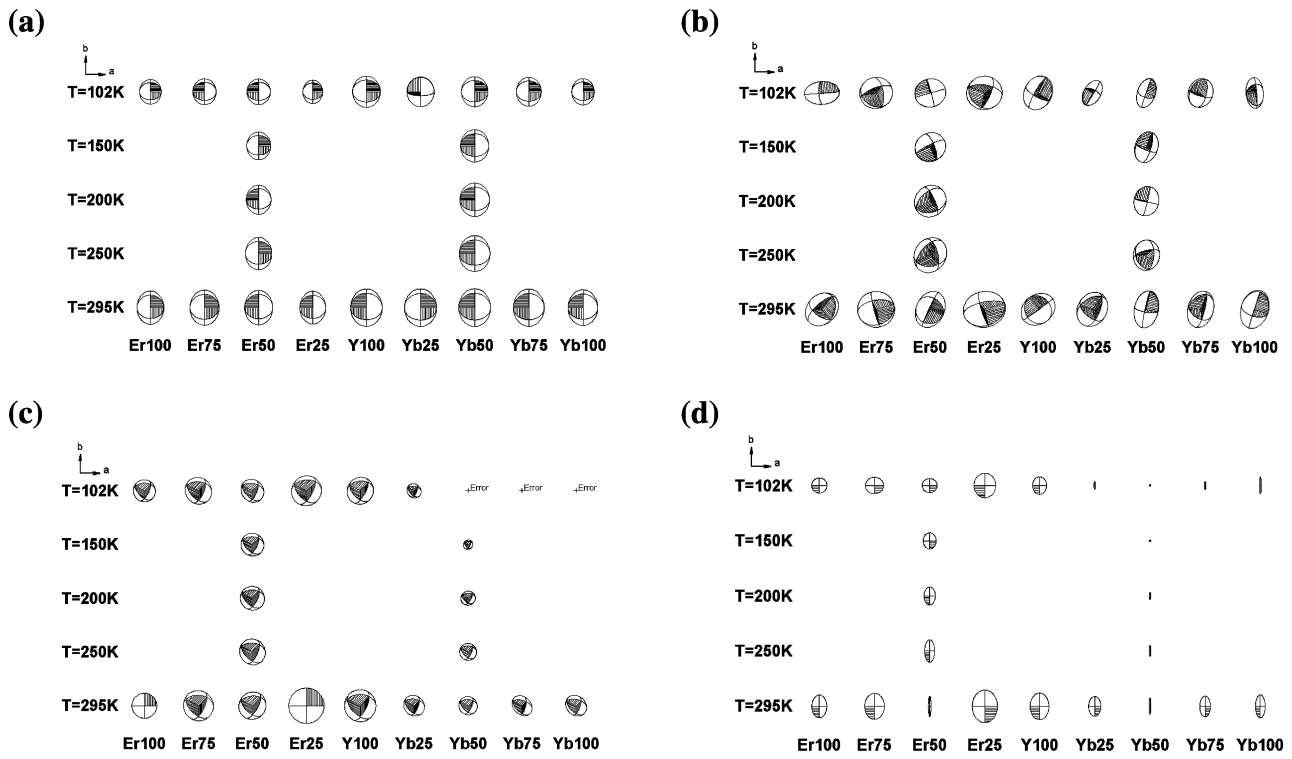

Figure 7. ADP ellipsoids at the 50% probability level for (a) dodecahedral cation, (b) oxygen ions, (c) Al(VI), and (d) Al(IV).

whereas the vibrations of the heavy ions are not connected with those of the light ones. The largest vibration amplitude of Er/Y/Yb overlaps with the smallest vibration amplitude of Al(VI), Al(IV), and O, Figure 8.

As one can see from the plot, there is an excellent agreement for the data collected at the two temperatures. The shape of the curves is almost the same for both temperatures for all four dependences U_{eq} vs concentration of lanthanide ions, although only two of them are illustrated in Figure 8. This plot also shows that the mean motions of ions at the dodecahedral site for Yb substituted garnets are bigger than those for the Er series. This is connected with the ionic radius of ytterbium ions, which is smaller than that of erbium ions. The ytterbium ion has more space to move at the dodecahedral site.

Influence of Measurement Conditions. Diffraction Angle. It is interesting in the case of such typical inorganic materials as garnets to examine how much the final results depend on diffraction angle (Figure 9) and on minimal and maximal diffraction angles. This is equivalent, more or less, to probing with the X-ray diffraction technique the core and valence electron densities of ions. This gives an idea how

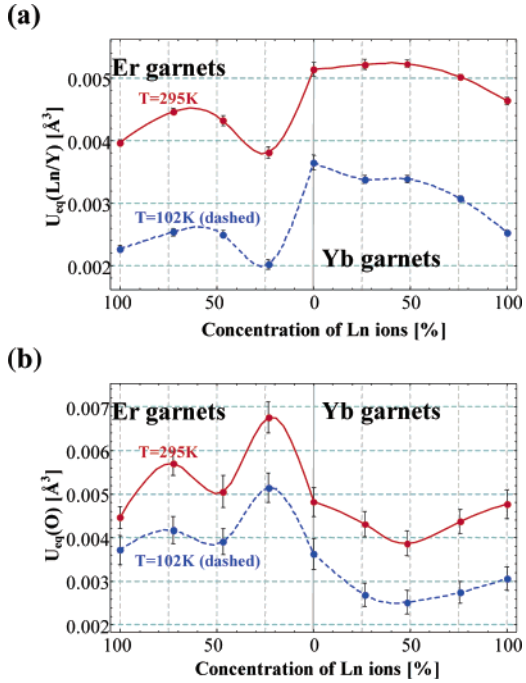

Figure 8. Cubic spline lines describing dependence of isotropic temperature factor, U_{eq}, of (a) Ln/Y and (b) oxygen ions vs concentration and temperature.

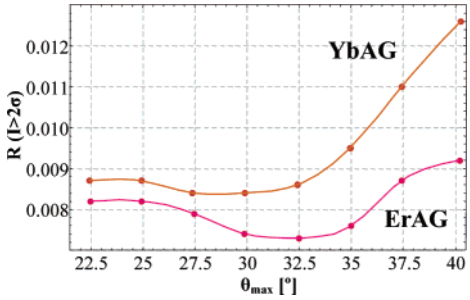

Figure 9. Cubic spline lines describing dependence of discrepancy *R*-factors on diffraction angle.

sensitive the measured structural parameters are to changes of experimental conditions. Such relations are obtained by using relatively high angle measurement results and then by a series of refinements with a maximal or minimal diffraction angle constrained to particular values.

Surprisingly enough it appears that the *R*-factors have clear minima for the maximal diffraction angles, θ_{max}, equal to 28 and 31° for the Er and Yb series (Figure 9), which suggests the best diffraction angles allowing the lowest discrepancy between the model and measured data.

In Figure 10 a,b, the dependence of the residual electron density on the diffraction angles is presented for both series. The difference between the residual electron densities ρ_{max} and ρ_{min} increases with increasing maximal diffraction angle, θ_{max}, and both dependences can be described by exponential functions. This means that weak high-angle reflections introduce significant errors to the data. The high-angle data are related to the core electron density, and for such densities we obtain exponential functions which can be expected on theoretical grounds. On the other hand, the dependence on the minimal diffraction angle, θ_{min}, is almost linear. The low-angle diffraction data can be related to the valence electron

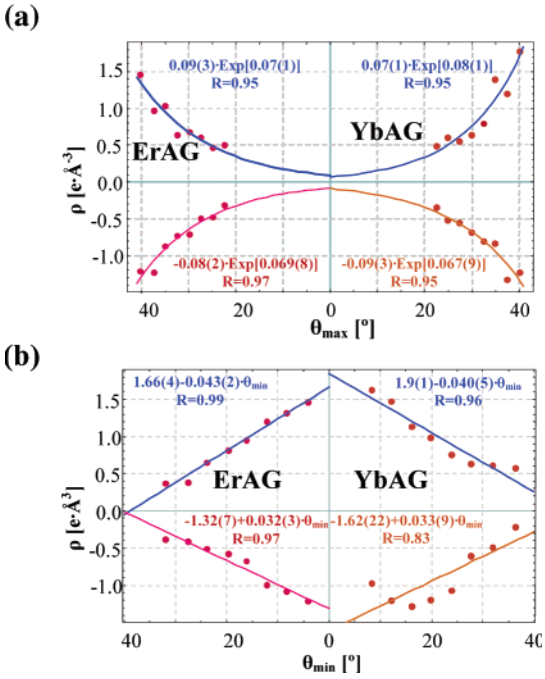

Figure 10. Dependence of ρ_{max} (positive values) and ρ_{min} (negative values) on (a) θ_{max} (for all four series of data points the functions describing the trends extrapolated to $\theta_{max} = 0°$) and (b) θ_{min} (for all four series of points the functions describing the trends adjusted and extrapolated to $\theta_{min} = 40°$).

density, and one would expect that this density far from nuclei can be approximated by a linear function. Of course, the residual electron densities depend very much on the diffraction angle. Increasing the maximal diffraction angle increases the residual peaks for a given structure. The reverse case is for the minimal residual electron density. In the case of higher minimal diffraction angle the differences between the maximal and minimal $\Delta\rho$ become smaller. Although the position of the oxygen ion only weakly depends on the diffraction angle, the coordinates of oxygen ions O_x and O_z do depend on it. The O_z coordinate decreases with increasing θ_{max}. It appears that d_{80} increases for both series of YAGs, whereas the d_8 distance decreases with increasing θ_{max}. The other two distances seem not to be dependent on the diffraction angle. Also, the temperature factors depend on the diffraction angle.

Discrepancy *R*-Factors. Discrepancy factors characterize the deviation of a given structural model from experimental data. For both series of garnets, the discrepancy factors change as a function of concentration of Er and Yb ions and temperature (Figure 11).

It appears that the best results of refinement are obtained for pure ErAG and YbAG (R_1 = ca. 1%) and the worst ones are for YAG and YAG crystals with small concentration of dopant. This is due to a substantial fluorescence coming from the yttrium ions. This influences the intensity of reflections, thus finally introducing a larger error. Another consequence of fluorescence for the yttrium rich samples is also the variation of the extinction coefficient. It resembles the dependence of the *R*-factor on concentration of doping ions and temperature. This coefficient compensates the decrease of intensity of reflections due to increasing fluorescence. There is almost no temperature dependence of the R_1-factor

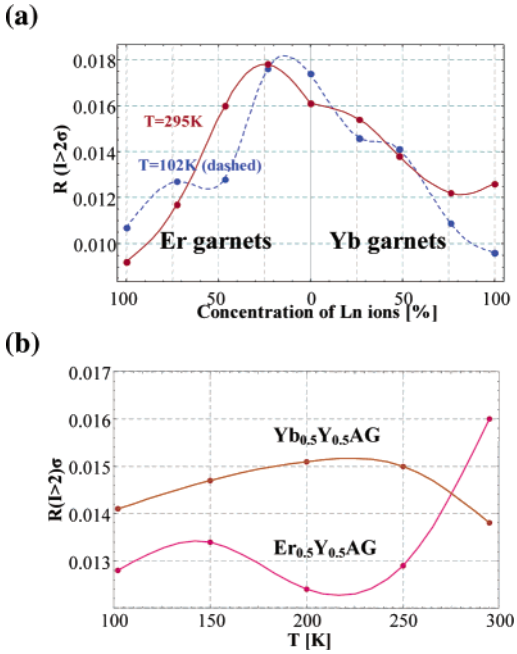

Figure 11. Cubic spline lines describing dependence of the discrepancy *R*-factor on (a) concentration of Er and Yb ions and (b) the temperature of measurements.

up to 250 K. Above this temperature, the R_1 value goes to ca. 1.8% for $Er_{0.5}Y_{0.5}AG$, whereas it goes down to 1.3% for $Yb_{0.5}Y_{0.5}AG$. Most of the R_1-factors are in the range from 1.25% up to 1.50% (for those reflections with intensities larger than two standard deviations). However, for all reflections, including the weakest ones, the final R_1-factors are ca. 3−4% and their dependences are similar to those already described when the criterion 2σ is applied.

Contrary to common expectations, there is not any systematic dependence of the R_1-factor on temperature. One could expect lower R_1-factors values for lower temperatures, but instead, the final results seem to be dependent on the scan step and the exposition time rather than on temperature. We just want to stress the role of optimization of experimental conditions.

Another important parameter characterizing the quality of refinement is the maximal residual electron density ($\Delta\rho_{max}$), which changes from ca. 0.8 e/Å^3 (for the pure YAG sample) up to 1.5 e/Å^3 for pure YbAG. There is a weak dependence of $\Delta\rho_{max}$ on the concentration of dopants—$\Delta\rho_{max}$ increases with increasing concentration of Er and Yb ions. This may be due to an increasing localization of charge for Er and Yb ions. The other reasons explaining this effect are inadequacy of the spherical model refinement and the Y/Ln disorder present in all these structures. There is no dependence of $\Delta\rho_{max}$ on temperature.

Approximated Electron Densities. As one can see from qualitative electron density maps, the electron density of ions at the dodecahedral sites is close to spherical (Figures 12 and 13).

The second minimum shell (from the center of these cations) could refer, in our opinion, to the ionic radii of Er, Y, or Yb in the solid state. There seems to be quite a reasonable agreement with the Shannon data. The first maximum ring could refer to 3d and 4f electron density clouds for Y and lanthanide ions, respectively.

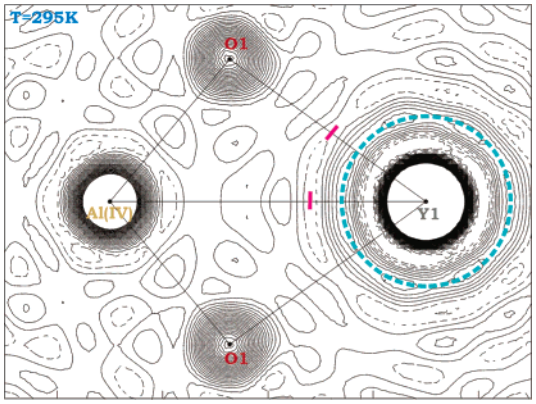

Figure 12. Electron density map for pure yttrium−aluminum garnet. Projection is toward the Y1−O1−Al(IV) plane.

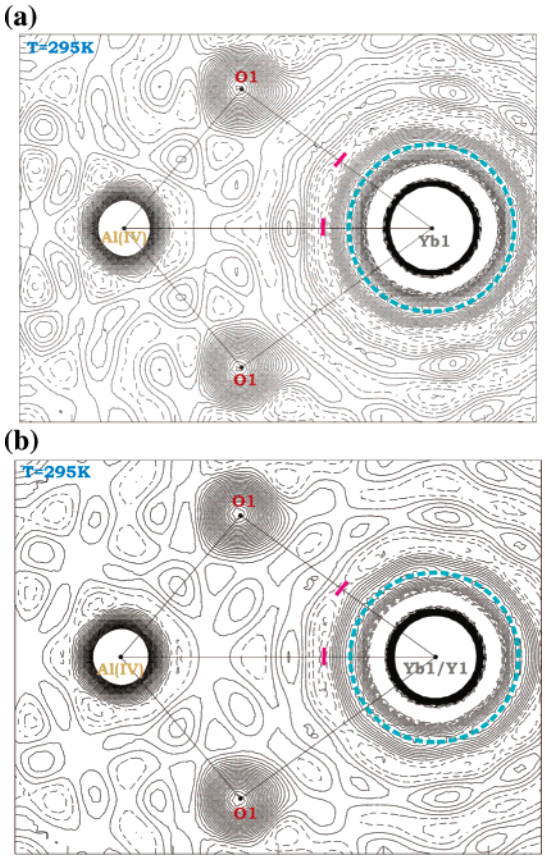

Figure 13. Electron density map for: (a) pure ytterbium−aluminum garnet; (b) Y/Yb aluminum garnet, with Yb (50 at. %), at $T = 295(2)$ K. Projection is toward the Y1/Yb1−O1−Al(IV) plane.

It will be interesting to compare such maps with those obtained from more rigorous electron density measurements and multipole refinement to see whether the minima and maxima around the dodecahedral sites are only within the experimental errors or they have a physical meaning. We continue working in this direction.

Analysis of Mixed (Er,Yb) Garnets. Linear dependencies for yttrium−aluminum and yttrium−erbium garnets allow studying the concentrations of both doping ions in mixed yttrium−erbium−ytterbium garnets provided one knows the

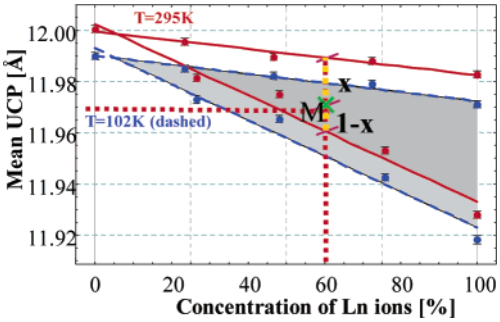

Figure 14. Idea for estimation of concentration of an unknown complex garnet knowing its unit cell parameters.

unit cell parameter of the mixed garnet and the amount of yttrium ions. The idea of such an analysis is given in Figure 14. Let us assume that one measured the averaged unit cell parameter of a mixed garnet and it is defined by point M in Figure 14. Then knowing the concentration of Y, one can calculate the ratio of concentrations of both doping ions $[x/(1 - x)]$. With the other condition defining the sum of concentrations of both ions, it is enough to calculate their individual concentrations.

Summary

We have grown and structurally characterized two series of YAG crystals doped with Er and Yb ions and analyzed the variation of their structural parameters. Structural data obtained are refined with some very low R_1-factors [$R(I > 2\sigma)$ from 0.92% to 1.78%]. The average unit cell parameters are, more or less, linearly dependent on the concentration of the doping/substituting ions. Although the unit cell parameters of substituted garnets seem to deviate slightly from the ideal cubic symmetry, some more precise powder and single-crystal measurements proved that the deviations from the cubic system are not significant.

The dependences of the absolute distance of the oxygen ion from the origin of the unit cell and the averaged unit cell parameter on the concentration of dopant are almost the same, showing clearly that *most of the changes in the structures come from the oxygen ion*, which is the only ion in the unit cell occupying general positions.

Changes of the unit cell parameters can be decomposed into the changes of particular interionic distances, which are mostly dependent on the position of oxygens. The oxygen ion is easily polarizable because of its size and relatively low electron density. Electron density maps indicate an unspherical shape of the oxygen anions. The higher concentration of the lanthanides, the higher the deformation of the oxygen ions.

The atomic displacement parameters of both types of aluminum ions are influenced by the motion of the oxygen ion. As can be expected, the much heavier Er, Y, and Yb ions are less mobile. The shape of the ADP ellipsoids for all cations is closely connected with their coordination numbers and the shapes of the voids occupied by a given ion. There is a clear correlation of the maximum amplitude of ADP ellipsoids of Er/Y/Yb ions with the minimum amplitude of ADP ellipsoids of Al(VI), Al(IV), and O. The mean motions of ions at the dodecahedral sites for Yb-substituted garnets are bigger than those for the Er series.

For both series of garnets, the deviation of the σ_o angle from the ideal octahedral value is around 2.5°, while the value of ϕ angle differs by more then 3°.

Considering the influence of measurement conditions on the final results, the following were recognized. The residual electron densities and the temperature factors depend on the diffraction angle. The maximal and minimal residual electron densities increase exponentially with increasing maximal diffraction angle and increase almost linearly with decreasing minimal diffraction angle. Also it occurs that for both series the *R*-factors have clear minima as a function of the maximal diffraction angles (28 and 31° for the Er and Yb series, respectively).

Experimental Section

Crystal Growth. All single crystals were grown by the Czochralski method at the Institute of Electronic Materials Technology. A conventional Czochralski apparatus, rf heating, and an iridium crucible were applied. High-purity oxide powders (99.999%), Y_2O_3, Al_2O_3, Yb_2O_3, and Er_2O_3, were used as starting materials. The growth atmosphere was nitrogen with a small amount of oxygen, in the case of YAG:Yb, to avoid Yb^{2+} ions. The crystals were seeded-grown in the [111] direction. Two series of crystals were obtained: one with Yb as dopant; the second one with erbium with approximate concentrations of lanthanide ions equal to 25, 50, 75, and 100 at. %. The concentration of substituting ions in YAG:Er crystals is the same as it was in the melt (distribution coefficient in this case is equal to 1). However, for YAG:Yb crystals the distribution coefficient equals 1.1 [14] and 1.3 [15] and a proper composition of melt had to be established in each case. The final concentration of dopants in crystals was determined by independent measurements described in the next paragraph.

Determination of Er and Yb. For the determination of exact concentrations of lanthanide ions Er and Yb (Ln/Y ratio) a JY 7-Plus Geo-plasma emission spectrometer (Jobin-Yvon, France) was used with a Paschen-Ringe polychromator with a 50-cm long Rowland circle with holographic gratings of 3600 gr/mm (linear dispersion 0.55 nm/mm in the 1st order). Instrumental operating conditions and parameters are given in Table 4S (Supporting Information).

The acid and other reagents were of analytical grade. A single-element stock solution containing 1.000 g/L of Er or Yb (Aldrich, Germany) was used for the preparation of calibration standards in 16% aqua regia. The data for the detection limit based on 6σ, where σ is the standard deviation of the signal produced by a blank solution (16% aqua regia), together with the spectral wavelengths for each element are given in Table 5S (Supporting Information).

The accuracy of the results was assessed by the use of certified reference materials: AGV-1 (Andesit); RGM1 (Rhynolite). The good agreement of the obtained results with the certified values for both elements proofs the validity of the analytical procedure. The precision of the results, based on the six independent determinations, was below 5%.

To perform accurate determinations, a mathematical algorithm was developed for spectral and nonspectral interference effects.[16]

(14) Swirkowicz, M.; Karas, A.; Jurkiewicz-Wegner, E.; Bajor, A.; Gala, M.; Lukasiewicz, T. *Int. Symp. 50th Anniv. Death Prof. Jan Czochralski*; Abstract No. 21.
(15) Monchamp, R. R. *J. Cryst. Growth* **1971**, *11*, 310.
(16) Jaroń, I.; Kudowska, B.; Bulska, E. *At. Spectrosc.* **2000**, *21*, 105.

Additionally the AC-E granite standard reference material, containing 14.7% of Al_2O_3, was used for the validation of the analytical procedure.

Single-Crystal X-ray Diffraction. All structural data were collected on a KM4CCD diffractometer with Mo Kα radiation and a graphite monochromator at two temperatures (295 and 102 K). Reflections from symmetry-related regions of the reciprocal lattice were collected. A spherical absorption correction was applied for a wide 2θ range of reflections (8−80°). To avoid unwanted effects ("$\lambda/2$ contamination", high absorption) small spherical crystals with a diameter of 0.22−0.30 mm were used. The "$\lambda/2$ contamination" phenomenon[17] is a serious problem which occurs for highly scattering materials (e.g. YAGs) on diffractometers equipped with a CCD (charge coupled device) detector. Because of single-crystal monochromatization of the X-rays, the radiation primary beam could be contaminated by photons with energy 2×, 3×, etc., higher than the starting Kα energy of a given X-ray tube anode. As a consequence, relatively weak artificial reflections are observed. This comes from the higher orders of diffraction. To avoid this effect, the X-ray tube acceleration voltage should be decreased—in the case of the Mo anode a pure primary X-ray beam is obtained for $U_{max} = 34.9$ kV— or some very small crystals used. A lower U lowers the energy of photons and, unfortunately, reduces the intensity of the characteristic radiation.

Small single crystals were positioned at 65 mm from the KM4CCD camera. The data were corrected for Lorentz and polarization effects. A spherical absorption correction was applied. Data reduction and analysis were carried out with the Kuma diffraction (Wrocław, Poland) programs (KM4CCD and KM4RED).

The structure was solved by direct methods[18] and refined using SHELXL.[19] The refinement was based on F^2 for all reflections except those with very negative F^2. Weighted R factors wR and all goodness-of-fit S values are based on F^2. Conventional R factors are based on F with F set to zero for negative F^2. The $F_o^2 > 2\sigma(F_o^2)$ criterion was used only for calculating R factors and is not relevant to the choice of reflections for the refinement. The R factors based on F^2 are about twice as large as those based on F. Scattering factors were taken from Tables 6.1.1.4 and 4.2.4.2 in ref 20.

Acknowledgment. The X-ray measurements were undertaken in the Crystallographic Unit of the Physical Chemistry Laboratory at the Chemistry Department of the University of Warsaw. K.W., D.A.P., and Z.F. are thankful for the Polish KBN support within Grant T07-12-501/66-1021GR.

Supporting Information Available: Crystal data and structural parameters for all crystals studied, as well as instrumental operating conditions for determination of Er and Yb, and CIF files. This material is available free of charge via the Internet at http://pubs.acs.org.

IC049920Z

(17) Kirshbaum, K.; Martin, A.; Pinkerton, A. A. *J. Appl. Crystallogr.* **1997**, *30*, 514.

(18) Sheldrick, G. M. *Acta Crystallogr., Sect. A* **1990**, *46*, 467.

(19) Sheldrick, G. M. *SHELXL93. Program for the Refinement of Crystal Structures*; University of Göttingen: Göttingen, Germany, 1993.

(20) *International Tables for Crystallography*; Wilson, A. J. C., Ed.; Kluwer: Dordrecht, The Netherlands, 1992; Vol. C.